Electric Polarization Properties of Single Bacteria Measured with Electrostatic Force Microscopy

Daniel Esteban-Ferrer,[†,⊥] Martin A. Edwards,[†,⊥] Laura Fumagalli,[*,†,‡] Antonio Juárez,[†,§] and Gabriel Gomila[*,†,‡]

[†]Institut de Bioenginyeria de Catalunya (IBEC), C/Baldiri i Reixac 11-15, 08028 Barcelona, Spain, [‡]Departament d'Electronica, Universitat de Barcelona, C/Marti i Franqués, 1, 08028 Barcelona, Spain, and [§]Departament de Microbiologia, Facultat de Biologia, Universitat de Barcelona, 08028 Barcelona, Spain. [⊥]D.E.-F. and M.A.E. contributed equally. The manuscript was written through contributions of all authors. All authors have given approval to the final version of the manuscript.

ABSTRACT We quantified the electrical polarization properties of single bacterial cells using electrostatic force microscopy. We found that the effective dielectric constant, $\varepsilon_{r,eff}$, for the four bacterial types investigated (*Salmonella typhimurium*, *Escherchia coli*, *Lactobacilus sakei*, and *Listeria innocua*) is around 3−5 under dry air conditions. Under ambient humidity, it increases to $\varepsilon_{r,eff} \sim 6-7$ for the Gram-negative bacterial types (*S. typhimurium* and *E. coli*) and to $\varepsilon_{r,eff} \sim 15-20$ for the Gram-positive ones (*L. sakei* and *L. innocua*). We show that the measured effective dielectric constants can be consistently interpreted in terms of the electric polarization properties of the biochemical components of the bacterial cell compartments and of their hydration state. These results demonstrate the potential of electrical studies of single bacterial cells.

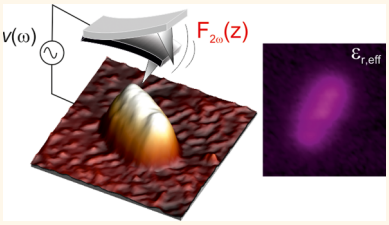

KEYWORDS: electrostatic force microscopy · single bacteria · dielectric constant · electric polarization · gram-type

The response of bacterial cells to external electric fields has previously been investigated using a variety of spectroscopic techniques, such as dielectric impedance spectroscopy,[1] dielectrophoresis spectroscopy,[2] and electrorotation spectroscopy.[3] These studies have revealed that the electrical response of bacteria depends on their shape and size, their internal structure, and the electric conductivity and permittivity of the different bacterial cell components, which may depend on the bacterial physiological state. Based on these results, the internal structure of a bacterial cell was inferred[4] and a number of electrical technologies were developed, including those to detect pathogenic bacteria,[5] to detect the presence of bacterial cells,[6] to count and differentiate bacteria,[7] to determine bacterial viability,[8] to distinguish among isogenic mutants,[9] and to separate bacteria from other cell sources.[10]

Most previous studies of the electrical properties of bacterial cells were carried out on bacterial populations of millions of cells. Only in the cases of electrorotation[3] and impedance cytometry[7] were single bacteria electrical measurements reported, but these had limited sensitivity and were based on complex electro-optical setups. Single cell measurements allow one to assess heterogeneity within a population and to perform measurements from a mixed sample without the need for separations. Recently, we demonstrated that electrostatic force microscopy (EFM) can be used to quantify the electrical properties of three-dimensional nano-objects, like nanoparticles and viruses, with high accuracy and reliability.[11] This technique therefore is an ideal candidate to address the study of the electrical properties of single bacterial cells.

Herein we show that EFM can be used to quantify the electric polarization response of single bacterial cells with high accuracy and reproducibility. We measured four bacterial cell types (*Salmonella typhimurium*, *Escherichia coli*, *Lactobacillus sakei*, and *Listeria innocua*), two of them Gram-negative (*S.* Typhimurium and *E. coli*) and two Gram-positive (*L. innocua* and *L. sakei*), in two environmental conditions, dry air (room temperature and <1% relative humidity (RH)) and ambient conditions (room temperature and >30% RH). We show that the effective dielectric constants obtained for the different bacterial types are well correlated with the intrinsic electric polarization properties

* Address correspondence to laura.fumagalli28@gmail.com, ggomila@ibecbarcelona.eu.

Received for review July 26, 2014 and accepted September 3, 2014.

Published online September 03, 2014
10.1021/nn5041476

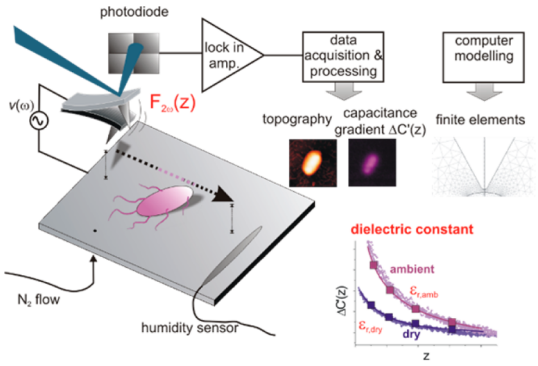

Figure 1. Schematic of measurement of the effective dielectric constant of a single bacterium using electrostatic force microscopy. Polarization force approach curves were obtained for each bacterium. The geometry of the bacterium was obtained from the topographic image. Finite-element numerical simulations of a homogeneous bacterium using the calibrated geometry of the probe were used to fit the experimental results and obtain the effective dielectric constant of the cell.

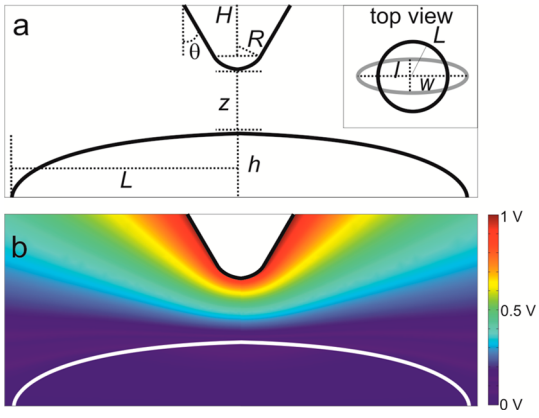

Figure 2. (a) Schematic representation of the tip sample system used in the finite element numerical calculations with the different input parameters indicated (drawing not to scale). The inset represents the top view with the black line showing the axisymmetric model that preserves the volume of the bacterium (gray line). (b) Example of a voltage distribution obtained for the case of a 200 nm high and 1.4 μm wide bacterial cell modeled as a solid oblate hemispheroid with effective dielectric constant $\varepsilon_{r,eff}$ = 6. Note: only part of the domain of simulation is shown.

of the biomolecular constituents and the hydration state of bacteria, thus opening interesting possibilities for further analytical studies of single bacteria.

RESULTS AND DISCUSSION

We measured the effective dielectric constant of single bacterial cells with EFM following the procedure recently developed for nanoparticles and single viruses,[11] as outlined schematically in Figure 1. Briefly, the electric polarization force between a bacterium and a nanometric conducting tip mounted on a force-sensing cantilever was measured at different positions while an alternating electric potential was applied between the tip and the underlying substrate. The dielectric constant was obtained by matching the experimental polarization force to that from a theoretical model in which the electrical properties of the bacterium were the changeable parameters. The model takes into account the sample and the probe geometries, which are obtained from topographic images and a tip calibration procedure, respectively (see Figure 2, and refs 11 and 12 for details).

Figure 3 shows the results of measurements performed on a single *S. typhimurium* cell in ambient conditions. The topographic image of the bacterium (Figure 3a) reveals the physical dimensions of this particular cell as l = 2 μm, w = 1 μm, and h = 205 nm, as can be seen more clearly from cross-sectional topographic profiles along the main axes of the bacterium (Figure 3b).

Electric polarization force images (shown as capacitance gradient images) of the same bacterial cell taken at increasing distances from the bacterium are shown in Figure 3c. As can be seen, the electrostatic force images clearly detect the presence of the bacterium with a contrast that decreases as the tip−bacterium distance increases. This is clearly evident in Figure 3d, which shows electric profiles taken along the cross section of the cell indicated in the electric images in Figure 3c. The maximum contrast ranges from 116 zF/nm at z = 20 nm from the cell to 15 zF/nm at z = 230 nm. These maximal dielectric contrast values as a function of distance are shown in Figure 3e as large squares. They were obtained by averaging the value of the electric signal on few pixels around the electric maximum and subtracting it from the value obtained by averaging the values in the same number of pixels on the electrode substrate. Note that the noise level of the measuring instrument is about ±5 zF/nm, thus giving an excellent signal-to-noise ratio in dielectric imaging up to distances of a few hundreds of nanometers from the cell. Figure 3e also shows contrast approach curves measured above the center of the bacteria (small dots corresponding to N = 12 curves). These curves agree with the dielectric contrast approach curves obtained from the dielectric images, thus validating the reliability and reproducibility of the dielectric measurements based on approach curves taken on the bacterial cell.

The solid line in Figure 3e represents the best-fit numerically calculated dielectric contrast curve, using R = 114 ± 4 nm, calculated as detailed in Materials and Methods (Supporting Information: S2), bacterial dimensions derived from the topography, and $\varepsilon_{r,eff}$ as the only variable. For these data, the best fit value was $\varepsilon_{r,eff} \sim 5.1 \pm 1.5$ where the error here represents the measurement standard deviation (as defined in the Materials and Methods section).

Figure 3f summarizes the values of $\varepsilon_{r,eff}$ as determined for five additional *S. typhimurium* cells using different tips. While the geometric parameters in each particular case are different (R = 81−160 nm,

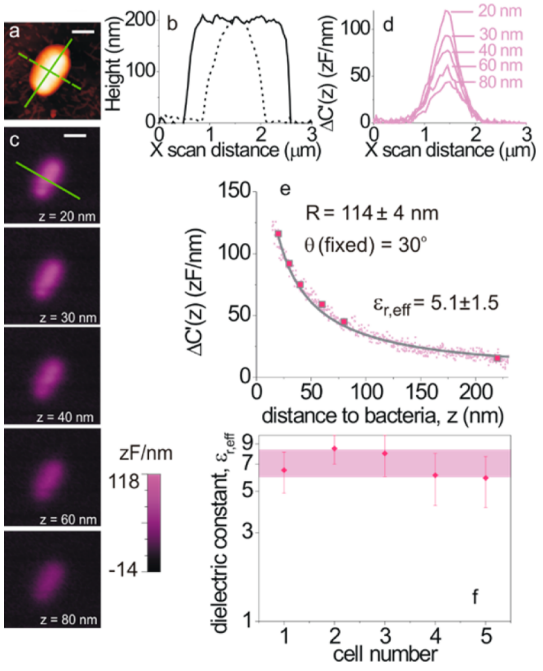

Figure 3. Measurement of the dielectric constant of a single *S. typhimurium* cell in ambient conditions. (a) Topography and (b) cross-sectional profiles of the cell analyzed (intermittent contact mode, free oscillation amplitude ~ 50 nm, set point ~ 70%, and resonance frequency ~ 95 kHz). (c) Capacitance gradient images and (d) cross-sectional profiles measured at different scan distances from the bacterium z = 20, 30, 40, 60, 80 ± 2 nm. Scale bar: 680 nm. (e) Capacitance gradient contrast approach curves (N = 12) measured on the center of the cell (pink dots). The filled symbols correspond to the maximum electric contrast obtained from the dielectric images in (c). The solid dark gray line is the fitted numerical calculation giving a dielectric permittivity of 5.1 ± 1.5 using a calibrated tip radius of 114 ± 4 nm and a oblate hemispheroid with h = 205 nm and L = 1.41 μm (extracted from the measured w = 1 μm and l = 2 μm). (f) Dielectric constants measured on n = 5 different *S. typhimurium* cells with different tips. The average value over the measured bacteria is $\varepsilon_{r,eff}$ = 7 ± 1.

h = 180−250 nm), the extracted dielectric constants lie in a narrow range of values for all the samples; thus, we can say that the effective dielectric constant is an intrinsic property of the bacterial cell, not dependent on geometrical factors, and that for *S. typhimurium* in ambient conditions it has a value $\varepsilon_{r,eff}$ = 7 ± 1 (error represents 1 standard deviation of the mean; for full details of all geometric parameters, see section S4 of the Supporting Information).

The same measurement procedure was repeated with the other cells types, the results of which are summarized in Table 1 (additional plots and geometric data and dielectric constant of each cell are reported in sections S3 and S4 in the Supporting Information).

In ambient conditions a strong correlation of the dielectric constant with the Gram-type is observed; namely, the Gram-positive bacteria (*L. sakei*, *L. innocua*) show relatively large values ($\varepsilon_{r,eff}$ ~ 18−19) while the Gram-negative bacteria (*S. typhimurium*, *E. coli*) show much smaller values $\varepsilon_{r,eff}$ ~ 6−7. Furthermore, we note

TABLE 1. Measured Mean Dielectric Constants of the Four Bacterial Types Analyzed in Ambient and Dry Conditions and Obtained from n = 5 Different Bacterial Cells in Each Case, Together with Its Mean Geometric Parameters (height and mean effective equatorial radius)

bacteria	Gram	$\varepsilon_{r,eff,amb}$	$\varepsilon_{r,eff,dry}$	h /nm	L /μm
S. typhimurium	−	7 ± 1	4.7 ± 1	212 ± 26	0.75 ± 0.06
E. coli	−	6.5 ± 1	3.3 ± 0.4	348 ± 34	0.9 ± 0.1
L. sakei	+	19 ± 5	3.3 ± 0.6	636 ± 40	1.1 ± 0.1
L. innocua	+	18 ± 7	3.7 ± 0.7	260 ± 33	0.7 ± 0.1

that within the Gram-type, different bacteria show remarkably similar values of dielectric constant, thus indicating a relatively small dependence on the bacterial type. While the absolute error for *L. sakei* and *L. innocua* is higher than that for the *S. typhimurium* and *E. coli*, the relative error is similar (~25%) because it is associated with the measurement error sources which are the same in both cases.

We next addressed the effect of relative humidity of the measured effective dielectric constant by reducing the humidity in the environmental chamber to a dry condition (<1% RH) and remeasuring the same cells. The values of the dielectric constants obtained under dry conditions are shown in Table 1 and as gray symbols in Figure 4a, whereas the cyan symbols represent the effective dielectric constants of the same cells measured under ambient conditions. The error bar represents the standard deviation over a set of N = 10−15 force curves measured on each bacterium. The colored bands are centered on the mean value for each bacterial type and their width represent plus minus one standard deviation which is also reported in Table 1. The effective dielectric coefficients measured in dry air conditions, $\varepsilon_{r,eff,dry}$, are significantly lower than those of the same bacteria measured in ambient conditions, $\varepsilon_{r,eff,amb}$. The change cannot be attributed to a change in the bacterial geometry, which remained unaltered, or to any significant effect of humidity in the tip radius which did not change (see section S5 in the Supporting Information). We therefore attribute the observed reduction in the dielectric constant upon drying to a modification of the dielectric properties of the bacterial cell itself.

We verified that these results were reversible for hydration/dehydration cycles as is shown in Figure 4b, where we plot the time evolution of the dielectric constants measured on a bacterium of each type when the environmental conditions were changed from ambient conditions to dry conditions (10 min) and back to ambient conditions (20 min).

The effective dielectric constant reported for each bacterial type, $\varepsilon_{r,eff}$, represents the electric polarization response of the whole cell under the influence of the external electric field generated by the sharp biased metallic probe. We consider the relationship of this parameter to the intrinsic dielectric constants of the

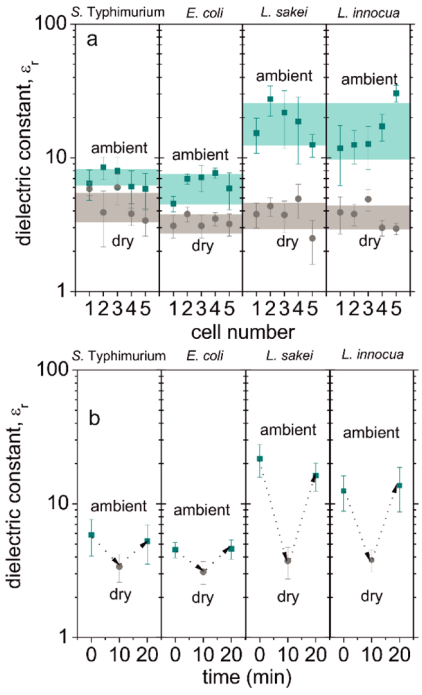

Figure 4. Measured mean dielectric constants of four types of bacterial cells analyzed in ambient (30−40% relative humidity, cyan squares) and dry air (<1% relative humidity, gray circles) conditions. Each of the $n = 5$ bacterial cells was measured in both conditions. The dielectric constant significantly reduces upon drying with a larger reduction for the case of Gram-positive bacteria. The color-coded regions indicate the obtained standard deviation of the values for each bacterium type under the different conditions (cyan for ambient and gray for dry conditions). (b) Evolution of the dielectric constant of single bacterial cells in a hydration/dehydration/rehydration cycle, analyzed for a single bacterium of each type.

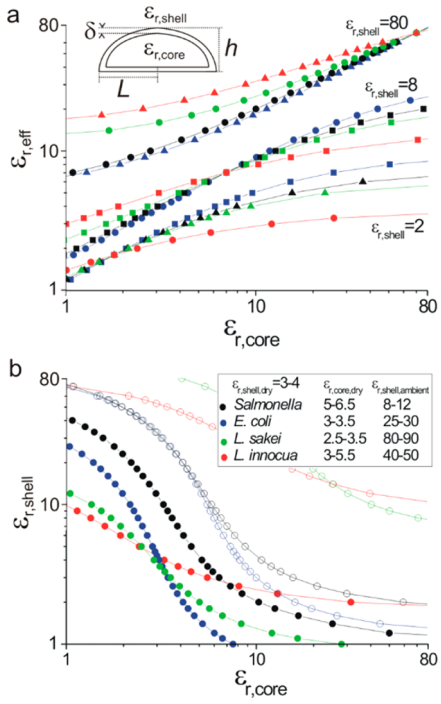

Figure 5. (a) Effective dielectric constant of a core−shell bacteria model for the four bacteria types investigated: *S. typhimurium* (black symbols), *E. coli* (blue symbols), *L. sakei* (green symbols), and *L. innocua* (red symbols) as a function of the dielectric constant of the core for three different dielectric constants of the shell, $\varepsilon_{r,shell} = 2$, 8, and 80. The dimensions of the bacteria correspond to the mean values reported in Table 1. The thickness of the shell for the Gram-negative bacteria is 25 nm, and for the Gram-positive, 60 nm. The tip radius is $R = 100$ nm, and the tip sample distance $z = 20$ nm. (b) Couples of values for $\varepsilon_{r,core}$ and $\varepsilon_{r,shell}$ compatible with the measured effective dielectric constants, $\varepsilon_{r,eff}$, for each bacterial type, in both dry (solid symbols) and ambient (empty symbols) conditions. Inset: Range of values for $\varepsilon_{r,core,dry}$ by assuming $\varepsilon_{r,shell,dry} = 3-4$, and range of values of $\varepsilon_{r,shell,ambient}$ by assuming $\varepsilon_{r,core,ambient} = \varepsilon_{r,core,dry}$.

different cell components using a simple core−shell model (see inset in Figure 5a for geometry), in which the core represents the cytoplasm region and the shell the bacterial envelope (which includes the plasma membrane, the cell wall, the periplasmic space, and, in the case of Gram-negative bacteria, the outer membrane).

We first note that the value of $\varepsilon_{r,eff}$ measured with EFM differs in general from the effective dielectric constant that would be obtained by considering an isolated core−shell bacteria in an uniform external electric field[13] (see section S6 in the Supporting Information). In our previous work with very small core−shell objects like viruses of ∼60 nm in diameter, the electric field was approximately uniform for the entirety of object and analytical models for uniform external electric fields could be used.[11] However, for a larger object like a bacterial cell, this is not the case and we must use numerical calculations to investigate the relation between $\varepsilon_{r,eff}$ and the dielectric constants of the cell components and its geometry.

In the core−shell bacterial model, the total thickness of the envelope of a Gram-negative bacteria was taken to be $\delta = 25$ nm, which lies within the characteristic range of values (20−30 nm), which includes the cell wall (2−7 nm thick), the outer membrane (7−8 nm), the periplasmic space (2−4 nm), and the cytoplasmatic membrane (7−8 nm). We did not include the external lipopolysaccharide chains, since they most probably disappeared during the sample preparation process. The thickness of the envelope of the Gram-positive bacteria was taken to be $\delta = 65$ nm, which is within the range of characteristic thicknesses for this type of bacteria (30−90 nm), which includes a much thicker cell wall (20−80 nm thick) but no outer membrane. Different dielectric constants were assigned to the shell and core, $\varepsilon_{r,shell}$ and $\varepsilon_{r,core}$, respectively, in order to account for a possible difference in their electric polarization response arising from their different biochemical composition. The bacterial sizes were taken as the mean values measured from the topography as reported in Table 1. The tip sample distance was taken as $z = 20$ nm and the probe radius $R = 100$ nm (the results are insensitive to these parameters; see section S7 in Supporting Information). Figure 5a shows the dependence of $\varepsilon_{r,eff}$ for the four bacteria types

investigated as a function of $\varepsilon_{r,core}$ for three characteristic values of $\varepsilon_{r,shell}$ = 2, 8, and 80.

In all cases, for a given $\varepsilon_{r,shell}$, the effective dielectric constant, $\varepsilon_{r,eff}$, increases with increasing $\varepsilon_{r,core}$ until a value of around 10 times $\varepsilon_{r,shell}$, at which it plateaus. This shows that $\varepsilon_{r,eff}$ includes contributions from both the envelope and the core of the bacterium, which is due to the long-range nature of the electrostatic forces. This is an important result, since it shows that although atomic force microscopy (AFM) is typically viewed as a surface technique, EFM is sensitive to the subsurface electric properties of the samples, in this case, the dielectric constant of the cytoplasm. We also note that for given $\varepsilon_{r,shell}$ and $\varepsilon_{r,core}$ the $\varepsilon_{r,eff}$ depends on the dimensions of the bacteria. These results show that $\varepsilon_{r,eff}$ depends on both the dimensions/structure of the bacterium and the dielectric properties of its constituent parts. Further simulations, where the probe dimensions and the tip−sample distance were varied over the range considered in this paper (R = 50−200 nm, z = 20−100 nm), determined that the calculated value of $\varepsilon_{r,eff}$ is independent of probe dimensions and it depends only weakly on the tip−sample distance (see section S7 in the Supporting Information for supporting data). Thus, $\varepsilon_{r,eff}$ can be considered an intrinsic parameter of the bacterium representing its effective electric polarization response, which includes both the electric polarization properties of the biochemical constituents and its geometry/internal structure.

For a fixed $\varepsilon_{r,eff}$ and geometry, there is a continuum possible of pairs of ($\varepsilon_{r,shell}$, $\varepsilon_{r,core}$) that would give rise to identical responses. Figure 5b shows sets of these pairs satisfying the experimentally measured $\varepsilon_{r,eff}$ for the four bacterial types and the two environmental conditions. As can be seen, there are a wide range of possible values for the core and shell dielectric constants that are compatible with the measured effective dielectric constants. However, in practice, this range can be reduced. In particular, we know that the envelope is mainly composed of proteins, lipids, and peptidoglycan, and that all these biomolecules are expected to show low electric polarization properties under dry conditions (around ∼2 for lipids[14] and ∼2−5 for proteins[15,16]). Therefore, a reasonable value for the shell dielectric constant under dry conditions can be chosen to be $\varepsilon_{r,shell,dry} \sim 3-4$.[16] Assuming this range of values for the shell under dry conditions, the corresponding dielectric constants for the cytoplasm are in the ranges $\varepsilon_{r,core,dry} \sim$ 5−6.5, 3−3.5, 2.5−3.5, and 3−5.5, for *S. typhimurium*, *E. coli*, *L. sakei*, and *L. innocua*, respectively. These values agree with the expected dielectric constants of the cytoplasm constituents (∼2−5 for proteins and ∼8−12 for nucleic acids[11,16]) and their relative proportions (roughly 3:1 proteins/nucleic acids dry weight).

Since the size of the bacterial cells did not change appreciably between the two environmental conditions, we assume that the cytoplasm remains unchanged and thus the dielectric constants of the core under ambient conditions are the same as those obtained from the analysis of the dry bacterial cells. Using these values, we obtain the dielectric constants for the shell in ambient conditions: $\varepsilon_{r,shell,ambient} \sim$ 8−12, 25−30, 80−90, and 40−50, for *S. typhimurium*, *E. coli*, *L. sakei*, and *L. innocua*, respectively. In all cases, we observe that the shell dielectric constants in ambient conditions are larger than the corresponding ones in dry conditions and are significantly larger than those assigned to the biomolecular constituents (∼2 for lipids and ∼2−5 for proteins).

These data suggest that the environmental humidity affects the dielectric response of the shell and that Gram-negative bacteria *S. typhimurium* and *E. coli* are less sensitive to changes in environmental humidity than the Gram-positive bacteria *L. sakei* and *L. innocua*. Structural differences between Gram-positive and Gram-negative bacteria that could cause this effect are (i) the presence of an outer membrane in Gram-negative cells, and (ii) the much thicker peptydoglycan layer in the Gram-positive bacteria. The outer membrane of Gram-negative bacteria is well-known as a permeability barrier for both hydrophobic and hydrophilic compounds. Nevertheless, it is considered that in bacterial cells the water permeability of bacterial membranes is high enough as to not require the presence of aquaporins for water transport.[17] Hence, we speculate that the hydration/dehydration of the multilayered peptidoglycan of *L. sakei* and *L. innocua* cells might account for the significant alteration of the dielectric constant of their shells when the environmental humidity is modified.

We cannot rule out, however, that this effect might also be the consequence of a global hydrophobic/hydrophilic difference between both types of cells. We remark that measuring the hydrophobic or hydrophilic nature of bacterial surfaces is of importance in the understanding of a number of biological processes, including adhesion, and that the molecular basis for the different behavior of Gram-positive and Gram-negative bacteria remains to be determined. Measuring the dielectric constant of bacterial cells using the approach outlined in this work, including assessing their response to the environment humidity, is therefore a promising route to evaluate critical biological properties of bacterial cells, such as adhesion, virulence, or viability.

Finally, we note that the dielectric constant values obtained for the bacterial envelope in ambient conditions are close to the values usually reported from measurements performed in liquid media by means of different macroscopic dielectric characterization techniques (refs 1−3 and 18). These values are in the order of ∼60 for the periplasm and ∼5−10 for the inner membrane and ∼10 for the outer membrane

(when present). This indicates that in dielectric measurements performed in fully hydrated bacteria water contributes significantly to the dielectric response and masks the intrinsic dielectric response from the biomolecular constituents. From an analytical point of view, therefore, using dry conditions offers the advantage to get rid of the effects of water in the dielectric characterization of bacterial cells, and to have direct access to the intrinsic electric polarization properties of biochemical constituents.

CONCLUSIONS

In this work, we have shown that electrostatic force microscopy can be used to measure the electric polarization properties of single bacterial cells in dry and ambient conditions. The effective dielectric constants of the cells obtained by assuming a homogeneous bacterial model revealed similar dielectric constants for the Gram-positive and Gram-negative bacteria in dry air conditions, $\varepsilon_{r,eff} \sim 3-5$. Under ambient conditions, larger values were systematically obtained for both groups; however, the increase was much larger for Gram-positive bacteria ($\varepsilon_{r,eff} \sim 18-19$) as compared to Gram-negative bacteria ($\varepsilon_{r,eff} \sim 6-7$). Analysis of the results obtained with a core−shell model revealed that the effective dielectric constant values obtained in dry air conditions are consistent with the dielectric response expected from its biochemical constituents (lipids, proteins, and nucleic acids) in dry conditions. In ambient conditions, the dielectric constant of the envelope significantly increases with respect to the dry values to $\varepsilon_{r,shell} \sim 10-30$ and $\varepsilon_{r,shell} \sim 40-80$ for the Gram-negative and Gram-positive bacteria, respectively. This change points toward a significant contribution of moisture, which has a larger impact in the Gram-positive than in the Gram-negative bacteria due to the thicker and more hydrophilic nature of their envelope. This work confirms that dielectric measurements of single bacterial cells can be correlated with the electric polarization response of their biochemical constituents and their internal structure, thus opening interesting possibilities for analytical studies based on the bacterial electric polarization properties.

MATERIALS AND METHODS

Electric Polarization Force Measurements. We measured the polarization force using dynamic EFM in amplitude detection.[11] Briefly, an ac voltage of amplitude, v_{ac}, and frequency, ω, was applied to the probe. The induced force oscillation at double the frequency, $F_{2\omega}$, was detected using a lock-in amplifier while taking dielectric images or approach curves (Figure 1). The capacitance gradient in the z-direction was then obtained using the relationship $C'(z) = 4F_{2\omega}(z)/{v_{ac}}^2$. The tip distance from the substrate was obtained taking into account the simultaneously measured mean deflection. The tip−bacteria distance, z, was obtained by subtracting the bacteria height from the tip−substrate distance. Electrical force curves were also measured on the bare metallic substrate, and it is the capacitance gradient contrast curves calculated as $\Delta C'(z) = C'_{bact}(z) - C'_{metal}(z + h)$ that we report in this work, where h is the height measured at the center of the bacterial cell.

Measurements were performed with a commercial atomic force microscope (Nanosurf, S.L.) connected to an external lock-in amplifier (Anfatec). Measurements were performed in an environmental chamber (Nanosurf) with humidity monitored with a humidity sensor (Rotronic AG). For dry conditions (RH < 1%), humidity was lowered with a N_2 flow, ambient conditions typically ∼30−40% RH, both at room temperature. We used highly doped diamond probes (CDT-FMR, Nanosensors) with a spring constant of ∼2−9 N/m, resonance frequency of ∼100 kHz, nominal radius of ∼100 nm, and half-cone angle of 30°. The spring constant for each tip was determined by the thermal noise method. The analysis of the data was performed using the WSxM software (Nanotec Electrónica S.L.) and custom analysis routines written in Matlab (The Mathworks, Inc.). Dielectric images were obtained with the built-in constant height mode of the AFM instrument. All data were obtained with v_{ac} = 5 V RMS at ω = 2 kHz. Images were obtained at a speed of 1 s/line and approach curves at a velocity of 0.6 μm/s.

Finite-Element Numerical Calculations. The expected force acting on the probe was calculated as a function of the tip−sample separation, geometry, and electrical properties of the bacterium by solving Poisson's equation using the commercial finite-element package Comsol Multiphysics 3.4, resulting in theoretical contrast curves $\Delta C'(z,\varepsilon_r)$ as a function of the effective dielectric constant of the bacteria. As in our previous work[11,12] the tip was modeled as a truncated cone of half angle, θ, with a hemispherical apex of radius, R, and cone height, H. The bacterial cell was modeled as an oblate hemispheroid with polar semiaxis (height), h, and equatorial semiaxis (half-width), L. The hemispheroid geometry was used instead of the full spheroid geometry because it better reproduced the geometry of the adsorbed bacterial cells (see Figure S1 in the Supporting Information). Moreover, a hemispheroid geometry was used instead of a (hemi)ellipsoid ((half)rod shape) geometry, as it is amenable to two-dimensional axisymmetric numerical routines and reduces the number of variables considered. However, for calculations with the tip above the center of the bacteria, the spheroid geometry resulted in almost identical forces to the ellipsoidal one (errors < 5%, data not shown), as long as the polar axis, h, is maintained and the equatorial axis of the hemispheroid, L, is taken so that the volume of the bacteria is preserved, *i.e.*, $L = 1/2(lw)^{1/2}$, where l and w are the cell width and length, respectively. A schematic representation of the system modeled together with a distribution of calculated electric potential is shown in Figure 2. Unless otherwise stated, the bacterial cell was modeled as a solid with no internal structure and with a homogeneous effective dielectric constant, $\varepsilon_{r,eff}$, and no conductivity.

Dielectric Constant Extraction. The (effective) homogeneous dielectric constant of the corresponding bacterial cell, $\varepsilon_{r,eff}$, was determined from the experimental capacitance gradient contrast curves, $\Delta C_{exp}'(z)$, by following the procedure developed previously.[11] First, the apex radius of the measuring probe, R, was determined by fitting numerically calculated approach curves to the experimental curves on a metallic substrate. In the fitting, the cone height and cone angle were kept fixed to their nominal values, θ = 30° and H = 15 μm, respectively (example of calibration curves and their theoretical fits are given in the Supporting Information in Figure S2). We found tip radii in the range 100−200 nm, consistent with their nominal values. Second, the bacterial cell geometry was determined from the AFM topographic image, from where its length, l, height, h, and width, w, were obtained and used to determine the equivalent oblate hemispheroid geometry used in the theoretical models. Finally, theoretical capacitance gradient contrast curves, $\Delta C'(z,\varepsilon_{r,eff}) = C'_{bact}(z,\varepsilon_{r,eff}) - C'_{metal}(z + h)$, were calculated for

different values of $\varepsilon_{r,eff}$ for the previously determined bacterium and probe geometries. These curves were then fitted to the experimental curves with $\varepsilon_{r,eff}$ taken as that which best fit the experiments. For each bacterium, a number $N = 10-15$ of experimental curves taken on the central region of the bacterium surface were analyzed. The reported values for $\varepsilon_{r,eff}$ correspond to the mean and standard deviation of the extracted values for the different curves. The main sources of error in the extracted dielectric constants come from the instrumental noise and the variability observed in the acquisition of multiple curves on a spot on a nonideal surface such a bacteria surface.

Bacterial Models and Sample Preparation. Four model bacteria with rod shape and similar dimensions when growing in liquid media ($\sim 2\ \mu m \times 1\ \mu m$) were analyzed. As examples of Gram-negative bacteria, we selected the well-studied *E. coli* strain MG1655 and the related genus Salmonella (*S. typhimurium* strain SV5015), which is an aethiologic agent of various infectious diseases. As examples of Gram-positive bacteria, we selected *L. sakei* strain SK1 and *L. innocua*.

A single colony from an agar plate was used to inoculate a plastic tube containing 2.5 mL of either Luria–Bertani broth (LB) (*S. typhimurium*, *E. coli*, *L. innocua*) or MRS agar broth (*L. sakei*). Cultures were incubated overnight in a 37 °C shaker at 250 rpm. Cells were pelleted by centrifugation and resuspended in 2.5 mL of Milli-Q (MQ) water by vortexing for 20 s. Then 100 μL of the *S. typhimurium* or *E. coli* suspension was deposited on a freshly cleaved highly oriented pyrolitic graphite (HOPG) 1 cm × 1 cm plate and left to dry in a flow hood. The sample was then rinsed five times with MQ water to remove any poorly adhered cells and left to dry. As the *L. sakei* and *L. innocua* cells adhered poorly, the samples were diluted 50-fold before depositing and the rinsing step was omitted. The HOPG substrate was attached to a 1.5 cm diameter magnet using silver paint, which was connected to the electrical ground of the atomic force microscope by a small wire.

Conflict of Interest: The authors declare no competing financial interest.

Supporting Information Available: Shape of adsorbed bacteria, tip radius calibration curves, measurements for *L. sakei*, detailed tables of data, effect of humidity in calibration, and comparison with uniform field formulas. This material is available free of charge *via* the Internet at http://pubs.acs.org.

Acknowledgment. The authors are grateful for financial support from the Spanish MEC under grant TEC2010-16844 and thank the members of microbial biotechnology and host–pathogen interaction group (IBEC) for their assistance in preparing the bacterial cultures.

REFERENCES AND NOTES

1. Asami, K.; Hanai, T.; Koizumi, N. Dielectric Analysis of *Escherichia coli* Suspensions in the Light of the Theory of Interfacial Polarization. *Biophys. J.* **1980**, *31*, 215–228.
2. Hölzel, R. Non-invasive Determination of Bacterial Single Cell Properties by Electrorotation. *Biochim. Biophys. Acta* **1999**, *1450*, 53–60.
3. Sanchis, A.; Brown, A. P.; Sancho, M.; Martínez, G.; Sebastián, J. L.; Muñoz, S.; Miranda, J. M. Dielectric Characterization of Bacterial Cells Using Dielectrophoresis. *Bioelectromagnetics* **2007**, *28*, 393–401.
4. Fricke, H.; Schwan, H. P.; Li, K.; Bryson, V. Dielectric Study of the Low-Conductance Surface Membrane in E. coli. *Nature* **1956**, *187*, 134–135.
5. Mannoor, M. S.; Zhang, S.; Link, A. J.; McAlpine, M. C. Electrical Detection of Pathogenic Bacteria *via* Immobilized Antimicrobial Peptides. *Proc. Natl. Acad. Sci. U.S.A.* **2010**, *107*, 19207–19212.
6. Yang, L.; Bashir, R. Electrical/electrochemical Impedance for Rapid Detection of Foodborne Pathogenic Bacteria. *Biotechnol. Adv.* **2008**, *26*, 135–150.
7. Bernabini, C.; Holmes, D.; Morgan, H. Micro-impedance Cytometry for Detection and Analysis of Micron-sized Particles and Bacteria. *Lab Chip* **2011**, *11*, 407–412.
8. David, F.; Hebeisen, M.; Schade, G.; Franco-Lara, E.; Di Berardino, M. Viability and Membrane Potential Analysis of Bacillus Megaterium Cells by Impedance Flow Cytometry. *Biotechnol. Bioeng.* **2012**, *109*, 483–92.
9. Castellarnau, M.; Errachid, A.; Madrid, C.; Juárez, A.; Samitier, J. Dielectrophoresis as a Tool to Characterize and Differentiate Isogenic Mutants of *Escherichia coli*. *Biophys. J.* **2006**, *91*, 3937–3945.
10. Park, S.; Koklu, M.; Beskok, A. Particle Trapping in High-Conductivity Media with Electrothermally Enhanced Negative Dielectrophoresis. *Anal. Chem.* **2009**, *81*, 2303–2310.
11. Fumagalli, L.; Esteban Ferrer, D.; Cuervo, A.; Carrascosa, J.; Gomila, G. Label-free Identification of Single Dielectric Nanoparticles and Viruses with Ultraweak Polarization Forces. *Nat. Mater.* **2012**, *11*, 808–816.
12. Fumagalli, L.; Gramse, G.; Esteban-Ferrer, D.; Edwards, M. A.; Gomila, G. Quantifying the Dielectric Constant of Thick Insulators Using Electrostatic Force Microscopy. *Appl. Phys. Lett.* **2010**, *96*, 183107.
13. Giordano, S. Dielectric and Elastic Characterization of Nonlinear Heterogeneous Materials. *Materials* **2009**, *2*, 1418–1479.
14. Pethig, R.; Kell, D. B. The Passive Electrical Properties of Biological Systems: Their Significance in Physiology, Biophysics and Biotechnology. *Phys. Med. Biol.* **1987**, *32*, 933–970.
15. Simonson, T. Electrostatics and Dynamics of Proteins. *Rep. Prog. Phys.* **2003**, *66*, 737–787.
16. Cuervo, A.; Dans, P. D.; Carrascosa, J. L.; Orozco, M.; Gomila, G.; Fumagalli, L. Direct Measurement of the Dielectric Polarization Properties of DNA. *Proc. Natl. Acad. Sci. U.S.A.* **2014**, 10.1073/pnas.1405702111.
17. Benga, G. Water Channel Proteins (Later Called Aquaporins) and Relatives: Past, Present, and Future. *Life* **2009**, *61*, 112–133.
18. Bai, W.; Zhao, K. S.; Asami, K. Dielectric Properties of *E. coli* Cell as Simulated by the Three-Shell Spheroidal Model. *Biophys. Chem.* **2006**, *122*, 136–142.